Z. Phys. C – Particles and Fields 45, 193–208 (1989)

Zeitschrift für Physik C Particles and Fields

Charged multiplicity distributions and correlations in e^+e^- annihilation at PETRA energies

TASSO Collaboration

W. Braunschweig, R. Gerhards, F.J. Kirschfink[1], H.-U. Martyn
I. Physikalisches Institut der RWTH, Aachen, Federal Republic of Germany[a]

H.-M. Fischer, H. Hartmann, J. Hartmann, E. Hilger, A. Jocksch, R. Wedemeyer
Physikalisches Institut der Universität, Bonn, Federal Republic of Germany[a]

B. Foster, A.J. Martin
H.H. Wills Physics Laboratory, University of Bristol, Bristol, UK[b]

E. Bernardi[2], J. Chwastowski[3], A. Eskreys[3], K. Gather, K. Genser[4], H. Hultschig, P. Joos, H. Kowalski[5], A. Ladage, B. Löhr, D. Lüke[6], P. Mättig[7], D. Notz, J.M. Pawlak[4], K.-U. Pösnecker, E. Ros, D. Trines, R. Walczak[4], G. Wolf
Deutsches Elektronen-Synchrotron DESY, Hamburg, Federal Republic of Germany

H. Kolanoski
Institut für Physik, Universität, Dortmund, Federal Republic of Germany[a]

T. Kracht[8], J. Krüger, E. Lohrmann, G. Poelz, W. Zeuner[9]
II. Institut für Experimentalphysik der Universität, Hamburg, Federal Republic of Germany[a]

J. Hassard, J. Shulman, D. Su
Department of Physics, Imperial College, London, UK[b]

F. Barreiro, A. Leites, J. del Peso
Universidad Autonoma de Madrid, Madrid, Spain[c]

M.G. Bowler, P.N. Burrows[10], M.E. Veitch
Department of Nuclear Physics, Oxford University, Oxford, UK[b]

G.E. Forden[11], J.C. Hart, D.H. Saxon
Rutherford Appleton Laboratory, Chilton, Didcot, UK[b]

S. Brandt, M. Holder
Fachbereich Physik der Universität-Gesamthochschule, Siegen, Federal Republic of Germany[a]

Y. Eisenberg, U. Karshon, G. Mikenberg, A. Montag, D. Revel, E. Ronat, A. Shapira, N. Wainer, G. Yekutieli
Weizmann Institute, Rehovot, Israel[d]

A. Caldwell[12], D. Muller[13], S. Ritz[12], D. Strom[14], M. Takashima[9], Sau Lan Wu, G. Zobernig
Department of Physics, University of Wisconsin, Madison, Wis., USA[e]

Received 6 April 1989

[1] Now at Lufthansa, Hamburg, FRG
[2] Now at Robert Bosch GmbH, Schwieberdingen, FRG
[3] Now at Inst. of Nuclear Physics, Cracow, Poland
[4] Now at Warsaw University[f], Poland
[5] On leave at Columbia University, NY, USA
[6] On leave at CERN, Geneva, Switzerland
[7] Now at IPP Canada, Carleton University, Ottawa, Canada
[8] Now at Hasylab, DESY
[9] Now at CERN, Geneva, Switzerland
[10] Now at MIT, Cambridge, MA, USA
[11] Now at SUNY Stony Brook, Stony Brook, NY, USA
[12] Now at Columbia University, NY, USA
[13] Now at SLAC, California, CA, USA
[14] Now at University of Chicago, Chicago, IL, USA

[a] Supported by Bundesministerium für Forschung und Technologie
[b] Supported by UK Science and Engineering Research Council
[c] Supported by CAICYT
[d] Supported by the Minerva Gesellschaft für Forschung GmbH
[e] Supported by US Dept. of Energy, contract DE-AC02-76ER000881 and by US Nat. Sci. Foundation Grant no INT-8313994 for travel
[f] Partially supported by Grant CPBP 01.06

Abstract. We report on an analysis of the multiplicity distributions of charged particles produced in e^+e^- annihilation into hadrons at c.m. energies between 14 and 46.8 GeV. The charged multiplicity distributions of the whole event and single hemisphere deviate significantly from the Poisson distribution but follow approximate KNO scaling. We have also studied the multiplicity distributions in various rapidity intervals and found that they can be well described by the negative binomial distribution only for small central intervals. We have also analysed forward-backward multiplicity correlations for different energies and selections of particle charge and shown that they can be understood in terms of the fragmentation properties of the different quark flavours and by the production and decay of resonances. These correlations are well reproduced by the Lund string model.

1 Introduction

In the present study we analyse the multiplicity distributions and correlations for the c.m.s. energy $14\,\text{GeV} \leqq \sqrt{s} = W < 46.8\,\text{GeV}$. This is an extension of our earlier studies [1, 2] and is based on much larger statistics for $\sqrt{s} \geqq 35\,\text{GeV}$ and an improved data correction procedure. We discuss the shape of the multiplicity distributions for single jets and complete events, their energy and rapidity dependence, forward-backward multiplicity correlations and their charge dependence.

The multiplicity distributions have been extensively studied in hadron-hadron interactions (see [3] and references therein) and found to be useful in understanding the reaction mechanism involved. This type of study has been extended to e^+e^- annihilation and yielded also interesting information, e.g. the rapid increase of particle multiplicity with energy found first by the TASSO Collaboration [4] can be interpreted as increasing contribution from gluon bremsstrahlung. Analysing the multiplicity distributions in different regions of phase space makes one less sensitive to the constraints due to conservation laws and allows one to probe different production mechanisms.

The paper is arranged as follows. In Sects. 2 to 4 we briefly review the experimental track and event selection criteria, describe the correction procedure and study the systematic errors. In Sect. 5 we discuss the energy dependence of the average charged multiplicity and in Sect. 6 the shape of the multiplicity distribution. Section 7 is devoted to the discussion of multiplicity scaling. Section 8 contains the analysis of forward-backward multiplicity correlations and is followed by the concluding remarks in Sect. 9.

2 Data selection

The data were taken with the TASSO detector at PETRA at centre of mass energies ranging from 14 to 46.8 GeV. Details of the experimental setup may be found elsewhere [5]. Hadronic events were measured in the central detector [6] using information on charged particles. The trigger required between 2 and 5 tracks (4 for most of the data) with polar angles θ measured w.r.t. the beam satisfying $|\cos\theta| < 0.82$ and with minimum transverse momentum p_t w.r.t. the beam of typically 0.32 GeV/c. After event reconstruction we accepted the tracks satisfying the following criteria:

- a track had to be reconstructed in three dimensions with $|d_0| < 5$ cm, where d_0 is the distance of closest approach to the nominal beam position,
- $|z_0 - z_v| < 20$ cm, where z_v is the z coordinate averaged over all tracks in the event and z_0 is the track coordinate at the point of closest approach to the beam position,
- $p_t > 0.1$ GeV/c,
- $|\cos\theta| < 0.87$.

Using only the selected tracks the events were demanded to obey the following requirements:

- at least 4 (5) accepted charged tracks at $W < 27$ GeV ($W \geqq 27$ GeV),
- dividing the event into hemispheres by a plane perpendicular to the sphericity axis the τ pair production candidates were selected and removed. For $W \leqq 16$ GeV 3 charged particles in one hemisphere and 1 in the other, for $W > 16$ GeV 3 charged particles in one hemisphere and 1 or 3 in the other were required and were considered as τ events if the effective mass of both particle systems was smaller than the τ mass (with π mass assumed for observed particles),
- for $W < 15$ GeV tracks were required in both hemispheres defined with respect to the beam axis and the absolute value of the sum of charges of the accepted tracks had not to exceed 3,
- z_v had to be not more than 6 cm away from the nominal interaction point,
- the sum ($\sum p_i \equiv \sum_i |p_i|$) of the particle momenta had to be $\sum p_i > 0.265 \cdot W$.

The most relevant cuts for this analysis were those on the charged particle multiplicity and on the sum of the particle momenta.

Events surviving the cuts were then checked for showering electrons and as a result 3% of them were rejected as Bhabha scattering events. The studied energy range was subdivided into four groups with the average values of $\langle W \rangle = 14$, 22, 34.8 and 43.6 GeV.

Table 1. Event variables. The first quoted error is statistical, the second systematic. The average number of charged kaons at 43.6 GeV was extrapolated from the data at lower energies assuming a constant ratio of the mean number of charged kaons to the average charged multiplicity

$\langle W \rangle$	14 GeV	22 GeV	34.8 GeV	43.6 GeV
# events	2704	1913	52832	8620
Complete event				
$\langle n_{ch} \rangle$	$9.30 \pm 0.06 \pm 0.41$	$11.30 \pm 0.08 \pm 0.46$	$13.59 \pm 0.02 \pm 0.46$	$15.08 \pm 0.06 \pm 0.47$
D	$3.07 \pm 0.04 \pm 0.28$	$3.55 \pm 0.06 \pm 0.36$	$4.14 \pm 0.01 \pm 0.39$	$4.59 \pm 0.04 \pm 0.37$
$\frac{\langle n_{ch} \rangle}{D}$	$3.03 \pm 0.05 \pm 0.31$	$3.19 \pm 0.06 \pm 0.35$	$3.28 \pm 0.01 \pm 0.33$	$3.28 \pm 0.03 \pm 0.28$
$\langle K^{\pm} \rangle$	1.20 ± 0.05	1.50 ± 0.15	1.76 ± 0.20	1.93 ± 0.30
from K_S^0	0.79 ± 0.07	0.80 ± 0.09	1.02 ± 0.04	0.97 ± 0.04
from Λ	0.17 ± 0.05	0.28 ± 0.06	0.28 ± 0.03	0.33 ± 0.04
Single hemisphere				
$\langle n_{ch} \rangle$	$4.63 \pm 0.03 \pm 0.30$	$5.64 \pm 0.04 \pm 0.31$	$6.78 \pm 0.01 \pm 0.33$	$7.58 \pm 0.03 \pm 0.37$
D	$2.06 \pm 0.02 \pm 0.16$	$2.39 \pm 0.03 \pm 0.18$	$2.78 \pm 0.01 \pm 0.22$	$3.11 \pm 0.02 \pm 0.21$
$\frac{\langle n_{ch} \rangle}{D}$	$2.24 \pm 0.03 \pm 0.23$	$2.36 \pm 0.03 \pm 0.22$	$2.44 \pm 0.01 \pm 0.23$	$2.44 \pm 0.02 \pm 0.20$

Table 2. Background contribution to the hadronic samples (%). The statistical error is negligible, when not given

$\langle W \rangle$	14 GeV	22 GeV	34.8 GeV	43.6 GeV
$\gamma\gamma$	0.3	0.6	0.9	1.1
τ pair	1.2	1.1	0.7	0.6
Beam-gas	0.5 ± 0.5	Negligible	Negligible	Negligible

The numbers of events in the corresponding samples are given in Table 1. The contamination from lepton pair production, $\gamma\gamma$ and beam-gas scattering events was estimated using the Monte Carlo calculations and was found [1, 7] to be small (see Table 2).

3 Correction procedure

The distributions presented below are the result of correcting the raw data for limited acceptance and resolution of the detector, limited efficiency of the track finding and applied cuts, and also for QED initial state radiation. The charged multiplicity distribution correction procedure was based on Monte Carlo events generated according to the Lund string model (α_s^2 matrix element) [8] for $\langle W \rangle \leqq 37$ GeV. For $\langle W \rangle > 37$ GeV we used the Webber cluster model [9] since it gave a better description of the raw data. In the Monte Carlo analysis all promptly produced charged particles and those produced in the decay of particles with lifetimes shorter than $3 \cdot 10^{-10}$ s were considered.

Since the determination of the charged multiplicity is rather sensitive to the above mentioned effects, two distinct steps were taken to correct the measured unnormalized charged multiplicity distribution – $N_{\text{obs.}}^{\text{exp.}}(n_0)$, where n_0 is the number of observed tracks. The first one was to correct for detector effects. It was performed using Monte Carlo events, which after the detector simulation [10] and track reconstruction [11] passed the selection criteria. For each such event the number of observed tracks n_0 (with distribution $N_{\text{obs.}}^{\text{MC}}(n_0)$) was compared to the number of tracks actually generated n_p (with distribution $N_{\text{obs.}}^{\text{MC}}(n_p)$). This comparison yielded the correction matrix $M(n_p, n_0)$ with elements defined as:

$$M(n_p, n_0) = \frac{\text{No. of events with } n_p \text{ tracks generated when } n_0 \text{ tracks were observed}}{\text{No. of events with } n_0 \text{ tracks observed}}.$$

This matrix relates $N_{\text{obs.}}^{\text{MC}}(n_0)$ to $N_{\text{gen.}}^{\text{MC}}(n_p)$ by:

$$N_{\text{gen.}}^{\text{MC}}(n_p) = \sum_{n_0} M(n_p, n_0) \cdot N_{\text{obs.}}^{\text{MC}}(n_0).$$

The second step was to correct for the presence of the QED initial state radiation which could result in a reduction of the nominal centre of mass energy and thus charged multiplicity. Therefore another set of correction factors was calculated according to the following formula:

$$C_F(n_p) = \frac{\rho_{\text{NR}}(n_p)}{\rho_{\text{gen.}}(n_p)}$$

where $\rho_{\text{NR}}(n_p)$ is the normalized multiplicity distribution for events generated at fixed c.m.s. energy without detector simulation and $\rho_{\text{gen.}}(n_p)$ is the distribu-

tion $N_{\text{gen.}}^{\text{MC}}(n_p)$ after normalization. These factors were generally close to 1.

Finally, the corrected multiplicity distribution $N_{\text{exp.}}^{\text{cor.}}(n_p)$ reads:

$$N_{\text{exp.}}^{\text{cor.}}(n_p) = C_F(n_p) \sum_{n_0} M(n_p, n_0) \cdot N_{\text{obs.}}^{\text{exp.}}(n_0).$$

One should note that in the case of the total charged multiplicity distribution the above procedure automatically fulfills the charge conservation requirement of an even number of tracks. The reconstructed numbers of events with $n_p \leqq 5$ are model dependent in such a correction procedure. The above procedure was applied to the multiplicity distributions both in full phase space and limited rapidity intervals.

For the analysis of single hemisphere multiplicity distributions and of forward-backward multiplicity correlations, a hemisphere was defined by a plane perpendicular to the sphericity axis and its association with forward or backward direction was chosen at random. The appropriate correction formalism for the analysis of forward-backward multiplicity correlations is a simple extension of the above described procedure so the corrected two-dimensional multiplicity distribution reads:

$$N_{\text{cor.}}^{\text{exp.}}(n_{Fp}, n_{Bp}) = C_F(n_{Fp}, n_{Bp}) \cdot \sum_{n_{F0}, n_{B0}=0} M(n_{Fp}, n_{Bp}, n_{F0}, n_{B0}) \cdot N_{\text{obs.}}^{\text{exp.}}(n_{F0}, n_{B0}),$$

where n_F, n_B are the numbers of particles produced in the forward or backward hemisphere.

4 Systematic errors

To estimate systematic errors on the central moments of the charged multiplicity distributions we took into account the following (in parentheses we quote the contribution to the systematic error of the average charged multiplicity measured at 34.8 GeV):

- the influence of different trackfinders (± 0.32),
- the contribution of τ pair production and $\gamma\gamma$ interactions (± 0.13),
- differences between our Monte Carlo generators (± 0.25),
- the influence of different detector simulations (± 0.18),
- the effect of the cut on the thrust axis – $|\cos\theta_{\text{thrust}}| < 0.75$ (± 0.07).

These contributions were added in quadrature (± 0.46). For more details see our previous publication [12].

5 Average charged multiplicity

The corrected charged multiplicity distributions are presented in Tables 3 and 4 for the whole event and single hemisphere, respectively. The quoted errors are calculated from the statistical error and from the correction procedure. The average charged multiplicity $\langle n_{\text{ch}} \rangle$ and the dispersion D of these distributions are given in Table 1. Decay products of K_S^0 and Λ are contained in all multiplicity distributions. The contribution of the charged kaons and the decay products

Table 3. Whole event charged multiplicity distribution $\frac{1}{N} \cdot \frac{dN}{dn_{\text{ch}}}$ (%)

n_{ch}	$\langle W \rangle = 14$ GeV	$\langle W \rangle = 22$ GeV	$\langle W \rangle = 34.8$ GeV	$\langle W \rangle = 43.6$ GeV
2	0.5783 ± 0.1800	0.1631 ± 0.0895	0.0447 ± 0.0455	0.0328 ± 0.0357
4	5.3986 ± 0.4449	1.7797 ± 0.2557	0.5733 ± 0.0759	0.3446 ± 0.1505
6	16.4745 ± 0.7230	7.8243 ± 0.5185	3.1675 ± 0.1424	2.2958 ± 0.2682
8	26.6517 ± 0.9146	16.7981 ± 0.7497	8.3797 ± 0.2133	5.1983 ± 0.3303
10	25.0602 ± 0.8596	22.9196 ± 0.8749	15.3130 ± 0.2897	10.7780 ± 0.4604
12	14.9795 ± 0.6175	21.5560 ± 0.8322	19.7927 ± 0.3349	15.7378 ± 0.5594
14	6.7216 ± 0.3885	14.5702 ± 0.6494	19.2450 ± 0.3312	17.7662 ± 0.5933
16	2.6178 ± 0.2336	8.2160 ± 0.4705	14.4335 ± 0.2843	16.4074 ± 0.5626
18	0.8703 ± 0.1306	3.6614 ± 0.2927	9.1819 ± 0.2231	12.3672 ± 0.4756
20	0.4682 ± 0.1159	1.6538 ± 0.1931	5.0623 ± 0.1627	8.6055 ± 0.3927
22	0.1463 ± 0.0606	0.5892 ± 0.1048	2.7161 ± 0.1189	5.2095 ± 0.2972
24	0.0262 ± 0.0208	0.1637 ± 0.0513	1.2348 ± 0.0803	2.9188 ± 0.2171
26	0.0067 ± 0.0097	0.0697 ± 0.0312	0.5173 ± 0.0519	1.3995 ± 0.1416
28		0.0355 ± 0.0253	0.1977 ± 0.0326	0.6002 ± 0.0934
30			0.0831 ± 0.0213	0.2374 ± 0.0592
32			0.0400 ± 0.0155	0.0591 ± 0.0265
34			0.0132 ± 0.0084	0.0264 ± 0.0182
36			0.0043 ± 0.0055	0.0047 ± 0.0091
38				0.0111 ± 0.0217

Table 4. Single hemisphere charged multiplicity distribution $\frac{1}{N}\cdot\frac{dN}{dn_{ch}}$ (%)

n_{ch}	$\langle W\rangle = 14$ GeV	$\langle W\rangle = 22$ GeV	$\langle W\rangle = 34.8$ GeV	$\langle W\rangle = 43.6$ GeV
0	0.6157 ± 0.0980	0.2812 ± 0.0520	0.1252 ± 0.0142	0.1189 ± 0.0285
1	3.8679 ± 0.2218	2.0135 ± 0.1603	0.9615 ± 0.0511	0.6682 ± 0.0814
2	9.5270 ± 0.3366	5.3329 ± 0.2446	2.7727 ± 0.0834	1.9985 ± 0.1266
3	16.9531 ± 0.4669	10.8590 ± 0.3716	6.4916 ± 0.1280	4.5684 ± 0.1942
4	19.7048 ± 0.5014	15.1301 ± 0.4462	10.3787 ± 0.1627	8.0933 ± 0.2617
5	18.7225 ± 0.4810	17.5128 ± 0.4880	13.9725 ± 0.1918	11.1637 ± 0.3131
6	13.6571 ± 0.3881	15.7342 ± 0.4468	14.8574 ± 0.1975	13.3177 ± 0.3461
7	8.4164 ± 0.2886	12.5570 ± 0.3874	14.4296 ± 0.1951	13.1853 ± 0.3421
8	4.4369 ± 0.1999	8.7552 ± 0.3082	11.5939 ± 0.1720	12.1098 ± 0.3252
9	2.1841 ± 0.1363	5.4471 ± 0.2332	8.7374 ± 0.1476	10.0522 ± 0.2907
10	1.0125 ± 0.0948	3.2668 ± 0.1760	5.9590 ± 0.1203	7.8876 ± 0.2520
11	0.4761 ± 0.0614	1.5372 ± 0.1161	3.9341 ± 0.0968	5.8080 ± 0.2130
12	0.2729 ± 0.0502	0.8243 ± 0.0840	2.5193 ± 0.0770	4.1115 ± 0.1760
13	0.1075 ± 0.0409	0.4259 ± 0.0589	1.5241 ± 0.0603	2.6213 ± 0.1357
14	0.0263 ± 0.0150	0.1901 ± 0.0399	0.8236 ± 0.0437	1.8627 ± 0.1146
15	0.0140 ± 0.0109	0.0774 ± 0.0237	0.4603 ± 0.0331	1.0597 ± 0.0845
16	0.0026 ± 0.0045	0.0404 ± 0.0184	0.2206 ± 0.0224	0.6019 ± 0.0628
17	0.0031 ± 0.0054	0.0149 ± 0.0101	0.1281 ± 0.0175	0.3987 ± 0.0523
18			0.0641 ± 0.0123	0.1976 ± 0.0352
19			0.0174 ± 0.0066	0.0908 ± 0.0238
20			0.0148 ± 0.0059	0.0458 ± 0.0163
21			0.0091 ± 0.0048	0.0191 ± 0.0115
22			0.0045 ± 0.0047	0.0092 ± 0.0080
23			0.0005 ± 0.0008	0.0079 ± 0.0065

of K_S^0 and Λ to the average charged multiplicity estimated using our data [13] is also given in Table 1.

The energy dependence of the average charged multiplicity is shown in Fig. 1 together with data of other e^+e^- experiments [14–19]. All these data were fitted with various parametrizations assuming a systematic error close to ours (~4%) for all other measurements:

- $\langle n_{ch}\rangle = a + b\cdot\ln(s) + c\cdot\ln^2(s)$ as suggested by the analysis of pp data [20]. The fit yielded $a = 3.235 \pm 0.106$, $b = -0.340 \pm 0.079$ and $c = 0.260 \pm 0.013$ with $\chi^2 = 111$ for 78 d.o.f. The solid curve in Fig. 1 shows the result of this fit;
- $\langle n_{ch}\rangle = a\cdot s^b$ as predicted by the fireball and hydrodynamical models for hadron-hadron interactions (see [21] and references therein). The fit gave $a = 2.241 \pm 0.035$ and $b = 0.252 \pm 0.004$ with $\chi^2 = 158$ for 79 d.o.f.;
- QCD calculations [22, 23] for the evolution of partons in the leading log approximation give $\langle n_{ch}\rangle = a + b\cdot\exp\left(c\cdot\sqrt{\ln\left(\frac{s}{Q_0^2}\right)}\right)$. Assuming $Q_0 = 1$ GeV the fit gave $a = 2.560 \pm 0.0096$, $b = 0.083 \pm 0.014$ and $c = 1.856 \pm 0.067$ with $\chi^2 = 118$ for 78 d.o.f. and is shown by the dashed curve in Fig. 1. We checked that a change of Q_0 from 0.1 to 1.4 GeV results in a variation of b and c of ~50%, while the fit quality remains practically unchanged. There exists a prediction [22] that the parameter c depends on the number of flavours N_f and $c = \sqrt{72/(33 - 2\cdot N_f)}$. The fit with Q_0 treated as a fit parameter and $N_f = 3$ for $W < 3.7$ GeV, $N_f = 4$ for $3.7 \leqq W < 10.5$ GeV and $N_f = 5$ above 10.5 GeV gave $a = 2.320 \pm 0.028$, $b = 0.075 \pm 0.001$ and $Q_0 = 0.563 \pm 0.007$ GeV with $\chi^2 = 125$ for 78 d.o.f.

All the above functions describe the data fairly well and differences between them are visible only at much higher energies ($W \sim 100$ GeV).

The energy variation of the ratio $\frac{\langle n_{ch}\rangle}{D}$ for the whole event distributions is shown in Fig. 2 together with the values measured by other experiments [15, 17, 19]. This ratio is about 3 and weakly energy dependent. The solid curve in Fig. 2 corresponds to a Poissonian shape of the multiplicity distribution and is seen to differ from the experimentally measured values. The ratio $\frac{\langle n_{ch}\rangle}{D}$ for the single hemisphere is also weakly energy dependent and increases slightly with $\sqrt{s}$. The ratio of $\frac{\langle n_{ch}\rangle}{D}$ for the whole event to that for the single hemisphere is approximately constant and is: 1.35 ± 0.03, 1.35 ± 0.03, 1.34 ± 0.01 and 1.35 ± 0.02 at 14, 22, 34.8 and 43.6 GeV, respectively.

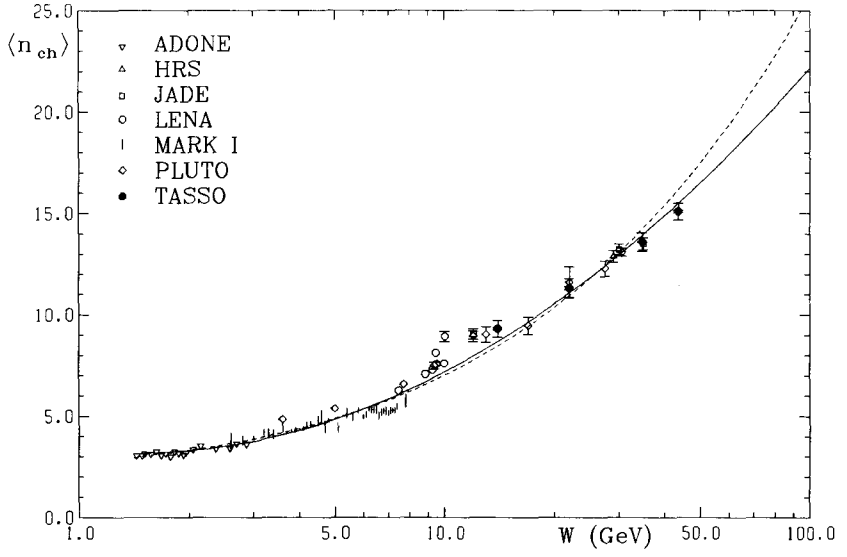

Fig. 1. Energy dependence of the average charged multiplicity. The curves show the fits to the data (see text). The statistical and systematic errors are shown for our data

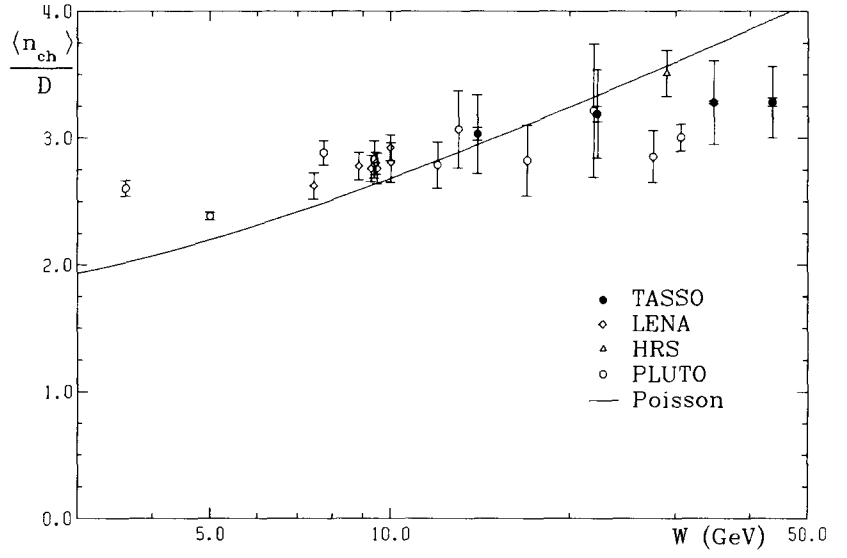

Fig. 2. Energy dependence of $\frac{\langle n_{ch}\rangle}{D}$. The systematic and statistical errors are shown for our data

These values are close to $\sqrt{2}$ which is expected for two jet events if the jets are produced independently.

6 Shape of the multiplicity distribution

There has recently been much interest in the shape of the multiplicity distributions at fixed centre of mass energy as well as their energy and rapidity dependence [3, 24]. The simplest distribution to be considered is the Poisson distribution. It would be valid if the final state particles were emitted independently and is expected in pure longitudinal phase space models [25].

In Fig. 3 the whole event charged multiplicity distributions at four centre of mass energies are shown. They are compared with the modified Poisson distribution (MPD-dashed curve):

$$\mathrm{MPD}(n_{ch}) = \begin{cases} 2\dfrac{\langle n_{ch}\rangle^{n_{ch}}}{n_{ch}!}e^{-\langle n_{ch}\rangle} & \text{if } n_{ch} \text{ even} \\ 0 & \text{otherwise} \end{cases}$$

and the latest Lund cascade model [26].

The MPD describes the data well at 14 and 22 GeV, but is too narrow at higher energies. This discrepancy becomes more pronounced with increasing $\sqrt{s}$. The Lund cascade model gives a good description of the data. We also checked that the charged multiplicity distributions of a single hemisphere cannot be satisfactorily reproduced by the Poisson distribution $\left(\mathrm{PD}(n_{ch}) = \dfrac{\langle n_{ch}\rangle^{n_{ch}}}{n_{ch}!}e^{-\langle n_{ch}\rangle}\right)$ – see Fig. 4. While

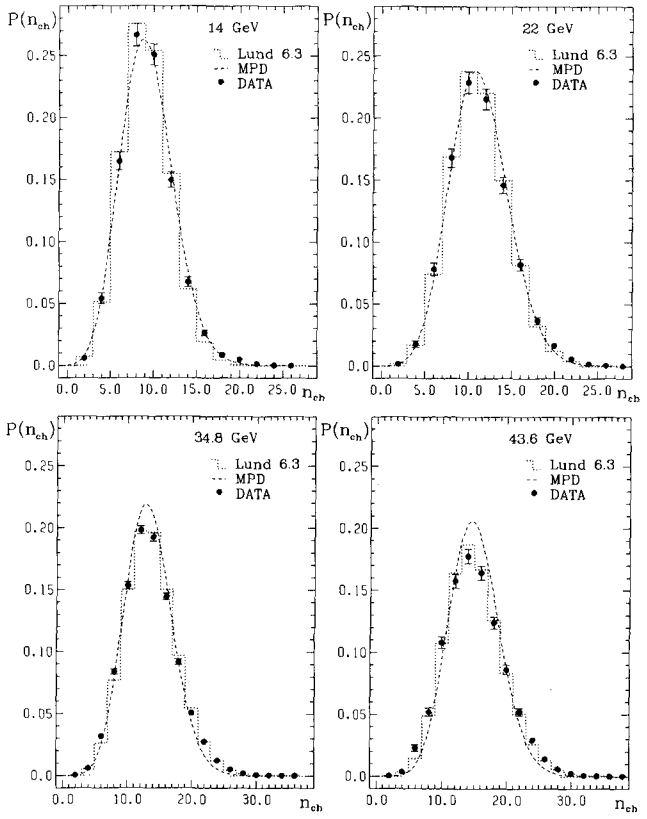

Fig. 3. Whole event charged multiplicity distribution compared with the modified Poisson distribution

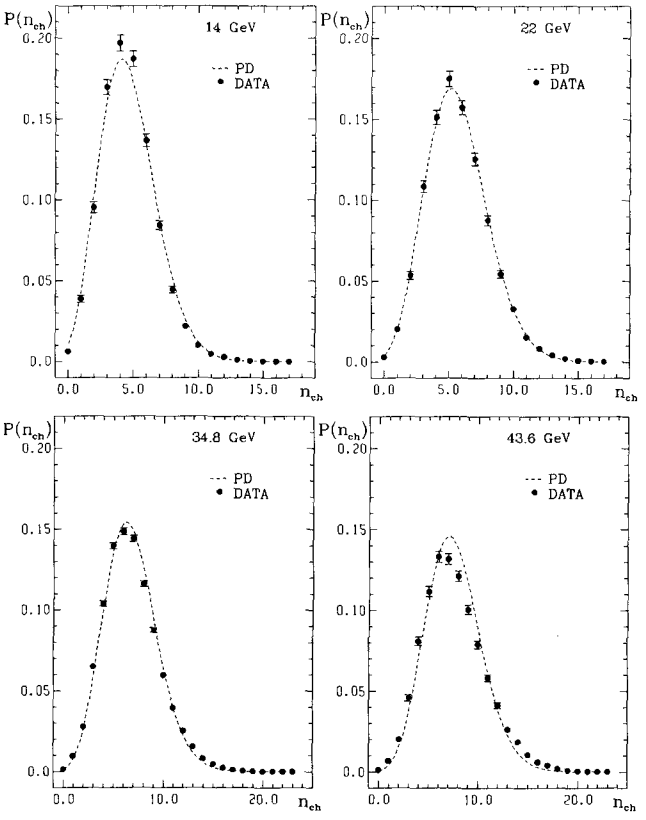

Fig. 4. Single hemisphere charged multiplicity distribution compared with the Poisson distribution

the PD is broader than the data at 14 GeV, it provides a good description at 22 GeV, but is too narrow at higher energies.

One of the most recently discussed distributions is the negative binomial distribution (NBD – see [24] and references therein):

$$\mathrm{NBD}(n, \langle n_{\mathrm{ch}}\rangle, k) = \frac{k(k+1)\ldots(k+n-1)}{n!}\left(\frac{\langle n_{\mathrm{ch}}\rangle}{\langle n_{\mathrm{ch}}\rangle + k}\right)^n \left(\frac{k}{\langle n_{\mathrm{ch}}\rangle + k}\right)^k.$$

where $\langle n_{\mathrm{ch}}\rangle$ and k are free parameters.

The dispersion of the negative binomial distribution D_{NB} is related to k and $\langle n_{\mathrm{ch}}\rangle$ by:

$$\frac{D_{\mathrm{NB}}^2}{\langle n_{\mathrm{ch}}\rangle^2} = \frac{1}{\langle n_{\mathrm{ch}}\rangle} + \frac{1}{k}. \tag{1}$$

The NBD was fitted to the charged multiplicity distributions measured in the full phase space and in limited parts of it for various interactions [19, 27–33] and generally it was found to provide a good description of the data. It has been argued [34] that the NBD should be fitted to the multiplicity distribution of particles of only one charge rather than to those of all particles since the former are not constrained by charge conservation. One should note that the above argument is of less importance in the case of multiplicity distributions measured in small regions of phase space. However, even in such restricted intervals some correlations due to charge conservation may be present.

In our case the NBD has been fitted to the whole event and single hemisphere multiplicity distributions and to the multiplicity distributions of negatively charged particles. The fits were performed for different rapidity intervals (rapidity was calculated w.r.t. the thrust axis assuming pion mass for a particle). The intervals had the width of $2 \cdot y_{\mathrm{cut}}$ and where centred symmetrically around zero. For the single hemisphere the interval extended from 0 to y_{cut}. The value of y_{cut} was varied from 0.5 to the maximum rapidity allowed for pions ($\sim$4.6, $\sim$5.1, $\sim$5.5, $\sim$5.75 at 14, 22, 34.8 and 43.6 GeV) in steps of 0.5. The fits to the multiplicity distributions of the whole event were carried out for intervals with $y_{\mathrm{cut}} < 2.5$ since for larger y_{cut} values the influence of charge conservation leads to the clear depletion of odd multiplicities.

In Fig. 5, the charged multiplicity distributions of the whole event are shown together with the best fits

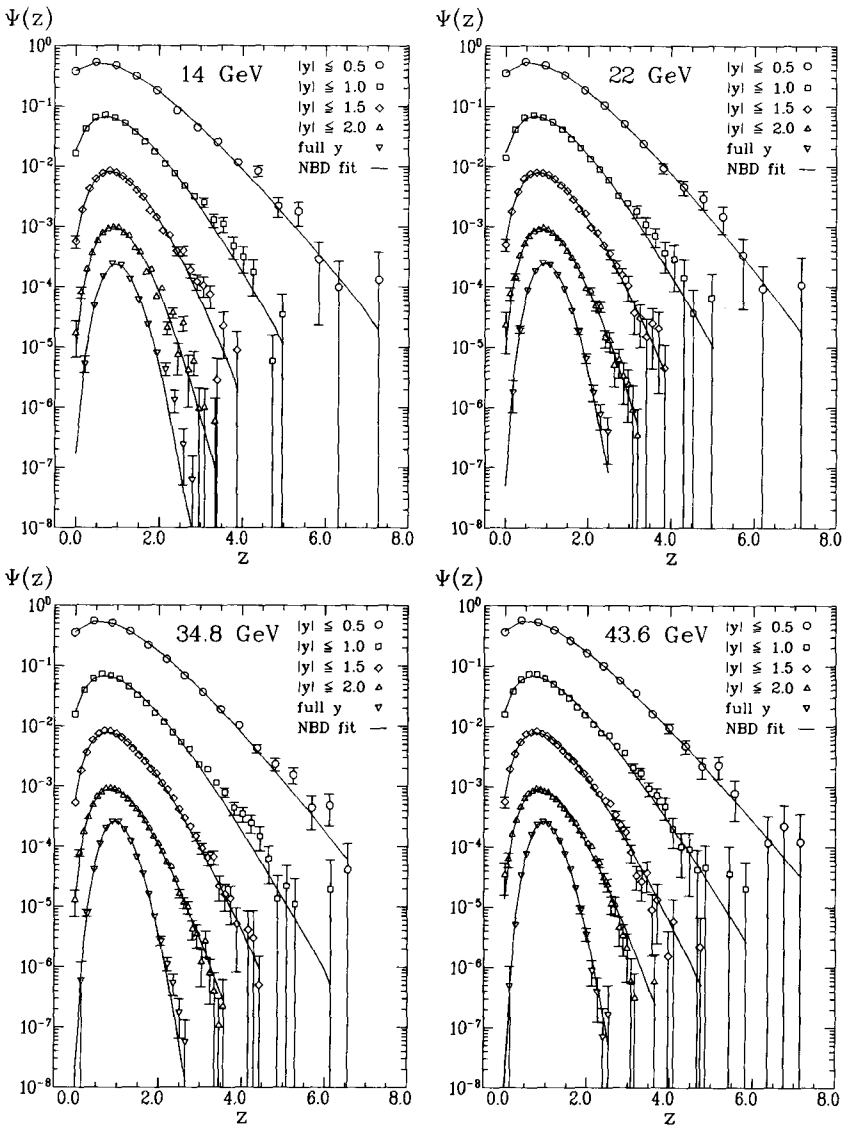

Fig. 5. Whole event charged multiplicity distributions in KNO form for different rapidity intervals. Each successive distribution is shifted down by one decade relative to the smaller interval

of the NBD using the KNO variables [35]: $\Psi(z) = \langle n_{ch} \rangle P(n_{ch})$ and $z = \frac{n_{ch}}{\langle n_{ch} \rangle}$, where $P(n_{ch})$ is the multiplicity distribution. The fitted values of $\langle n_{ch} \rangle$ and k^{-1} for the whole event distributions are compared in Table 5 with those calculated from the data using (1). The quoted errors on parameters are statistical only. The values of $\langle n_{ch} \rangle$ and k^{-1} fitted and those calculated from the data agree quite well. However, the quality of the fits, especially at 34.8 GeV where our data sample is the largest, is marginal. Moreover, the NBD fails to describe either the multiplicity distributions of negatively charged particles or the one hemisphere multiplicity distributions – see Table 6.

In Figs. 6–7 the rapidity and energy dependence of k^{-1} is presented and compared with those obtained by HRS [19], NA22 [31] and EMC [32] Collaborations. For a fixed rapidity interval the value of k^{-1} increases with growing $\sqrt{s}$. At a given energy, k^{-1} increases with decreasing y_{cut}, which together with a decrease of $\langle n_{ch} \rangle$ corresponds to a broadening of the KNO plot. This fact was predicted by Białas and Hayot [36] (for e^+e^- annihilation) as a sign of decreasing influence of overall energy-momentum conservation as the central rapidity interval is made smaller. This was also reproduced by models of the authors of [37] (e^+e^- annihilation) and of Fiałkowski [38] (hadron-hadron interactions). For each rapidity interval values of k^{-1} obtained by the HRS Collaboration are smaller than those resulting from the fits to our data at comparable energies, which means that the multiplicity distributions of HRS are narrower than ours (see also Fig. 9).

There are several theoretical approaches which

Table 5. Comparison of the fitted and calculated k^{-1} and $\langle n_{ch} \rangle$ for the whole event charged multiplicity distributions

$\langle W \rangle$ (GeV)	y_{cut}	Data		Fit		
		k^{-1}	$\langle n_{ch} \rangle$	k^{-1}	$\langle n_{ch} \rangle$	χ^2/N_{df}
14	0.5	0.239 ±0.035	2.06±0.03	0.226 ±0.026	2.04±0.03	15/13
	1.0	0.195 ±0.020	4.23±0.05	0.178 ±0.009	4.18±0.04	27/19
	1.5	0.121 ±0.014	6.21±0.06	0.105 ±0.006	6.13±0.04	33/22
	2.0	0.059 ±0.010	7.77±0.06	0.046 ±0.004	7.67±0.04	75/24
	full	0.0017±0.0072	9.30±0.06	−0.0017±0.0028	9.24±0.06	22/11
22	0.5	0.208 ±0.039	2.10±0.04	0.204 ±0.017	2.09±0.03	4/13
	1.0	0.194 ±0.024	4.42±0.07	0.179 ±0.012	4.39±0.03	19/20
	1.5	0.137 ±0.017	6.76±0.08	0.135 ±0.007	6.74±0.05	8/25
	2.0	0.083 ±0.013	8.76±0.09	0.078 ±0.004	8.76±0.06	13/27
	full	0.0099±0.0080	11.30±0.08	0.0099±0.0023	11.30±0.06	10/12
34.8	0.5	0.240 ±0.007	2.29±0.01	0.228 ±0.007	2.28±0.01	22/14
	1.0	0.220 ±0.005	4.73±0.01	0.201 ±0.004	4.68±0.02	102/25
	1.5	0.166 ±0.003	7.22±0.02	0.166 ±0.003	7.20±0.02	74/30
	2.0	0.113 ±0.003	9.56±0.02	0.112 ±0.003	9.55±0.03	27/33
	full	0.019 ±0.002	13.59±0.02	0.018 ±0.001	13.56±0.01	38/16
43.6	0.5	0.296 ±0.022	2.52±0.03	0.289 ±0.014	2.51±0.03	8/16
	1.0	0.252 ±0.014	5.15±0.04	0.240 ±0.007	5.13±0.03	44/26
	1.5	0.193 ±0.010	7.82±0.06	0.185 ±0.005	7.77±0.05	39/31
	2.0	0.134 ±0.008	10.43±0.06	0.126 ±0.004	10.38±0.05	39/33
	full	0.027 ±0.004	15.08±0.06	0.026 ±0.002	15.08±0.06	7/17

Table 6. Comparison of the fitted and calculated k^{-1} and $\langle n_{ch} \rangle$ at 34.8 GeV

y_{cut}	Data		Fit		
	k^{-1}	$\langle n_{ch} \rangle$	k^{-1}	$\langle n_{ch} \rangle$	χ^2/N_{df}
Single hemisphere multiplicity distributions					
0.5	0.249±0.009	1.14±0.01	0.241±0.008	1.14±0.01	217/10
1.0	0.278±0.005	2.38±0.01	0.245±0.001	2.36±0.01	216/17
1.5	0.227±0.004	3.64±0.01	0.213±0.002	3.63±0.01	215/20
2.0	0.156±0.003	4.81±0.01	0.153±0.002	4.81±0.01	57/22
2.5	0.096±0.002	5.75±0.01	0.096±0.002	5.75±0.01	37/22
3.0	0.056±0.002	6.34±0.01	0.055±0.002	6.34±0.01	43/22
3.5	0.034±0.002	6.63±0.01	0.034±0.001	6.63±0.01	44/22
4.0	0.025±0.002	6.74±0.01	0.023±0.001	6.74±0.01	64/22
4.5	0.021±0.002	6.77±0.01	0.019±0.001	6.77±0.01	89/22
full	0.020±0.002	6.78±0.01	0.018±0.001	6.78±0.01	103/22
Multiplicity distributions of negatively charged particles					
0.5	0.100±0.011	1.15±0.01	0.094±0.011	1.14±0.01	19/9
1.0	0.099±0.006	2.36±0.01	0.086±0.005	2.34±0.01	92/13
1.5	0.068±0.004	3.61±0.01	0.064±0.003	3.60±0.01	99/15
2.0	0.028±0.003	4.78±0.01	0.027±0.003	4.77±0.02	34/17
2.5	−0.008±0.002	5.74±0.01	−0.008±0.002	5.73±0.02	24/17

lead to a negative binomial type of multiplicity distribution (for a review see [24]). In some of them the parameter k is interpreted as the number of sources emitting particles. If this is the case our data seem to contradict these models since k is much larger than the average multiplicity and decreases with increasing energy.

7 Multiplicity scaling

An energy independent parametrization of the multiplicity distributions was proposed by Koba, Nielsen and Olesen [35]. Assuming Feynman scaling [39] they derived for $s \to \infty$ that the normalized moments of the distributions:

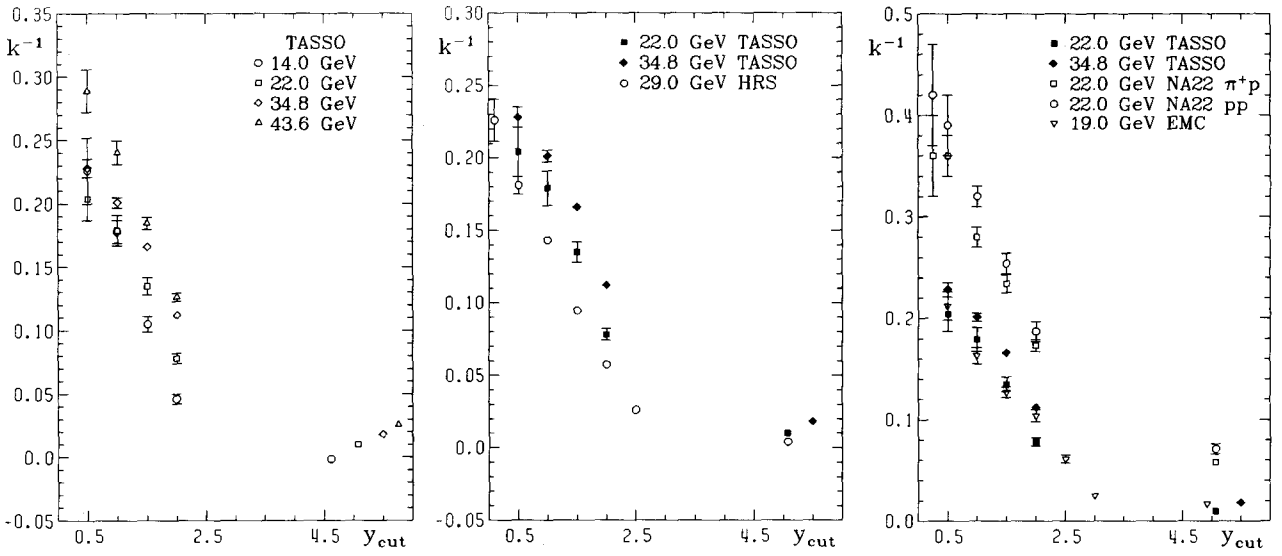

Fig. 6. Rapidity dependence of k^{-1} resulting from fits to the whole event charged multiplicity distributions

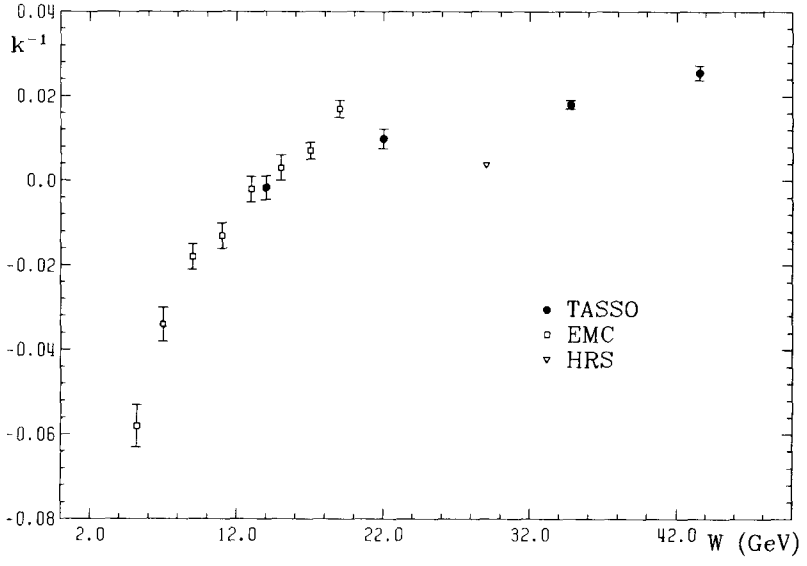

Fig. 7. Energy dependence of k^{-1} resulting from fits to the whole event charged multiplicity distributions

$$C_l = \frac{\langle n_{ch}^l \rangle}{\langle n_{ch} \rangle^l} \qquad (2)$$

are independent of both energy and $\langle n_{ch} \rangle$ but may depend on the interaction type. From the above it follows that the multiplicity distributions measured at different energies should coincide when plotted using variables $z = \frac{n_{ch}}{\langle n_{ch} \rangle}$ and $\Psi(z) = \langle n_{ch} \rangle P(n_{ch})$.

Experimentally the KNO-scaling was found to work approximately over a large energy interval in hadron-hadron interactions, and fails only at the highest presently available energies [40].

In Fig. 8 our charged multiplicity distributions together with those measured by PLUTO [17] at 3.6, 5 and 7.7 GeV and HRS [19] at 29 GeV are shown using the KNO variables. The data exhibit approximate KNO-scaling, although a slight tendency of the KNO distribution to narrow with increasing energy can be observed. The same holds if one studies single hemisphere multiplicity distributions (see Fig. 9).

A functional form of $\Psi(z) = \frac{81}{64}\pi^2 z^3 e^{-\frac{9}{16}\pi z^2}$ proposed by Barshay and Yamaguchi [41] was compared with the multiplicity distributions of the whole event and it proved to be incompatible with the data – see curve in Fig. 8.

The energy variation of the normalized moments C_l of whole event and single hemisphere multiplicity distributions is shown in Fig. 10a and b, respectively. The values of C_l are slightly decreasing with $\sqrt{s}$ (narrowing of the KNO distribution) and above 5 GeV are indeed almost energy independent, confirming approximate scaling.

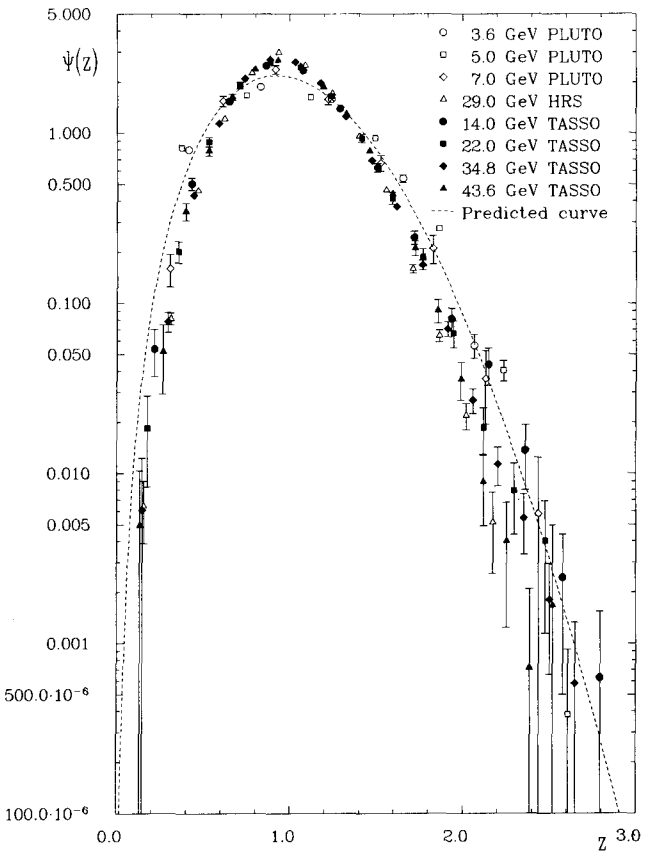

Fig. 8. Whole event charged multiplicity distributions in KNO form. Curve of [41]

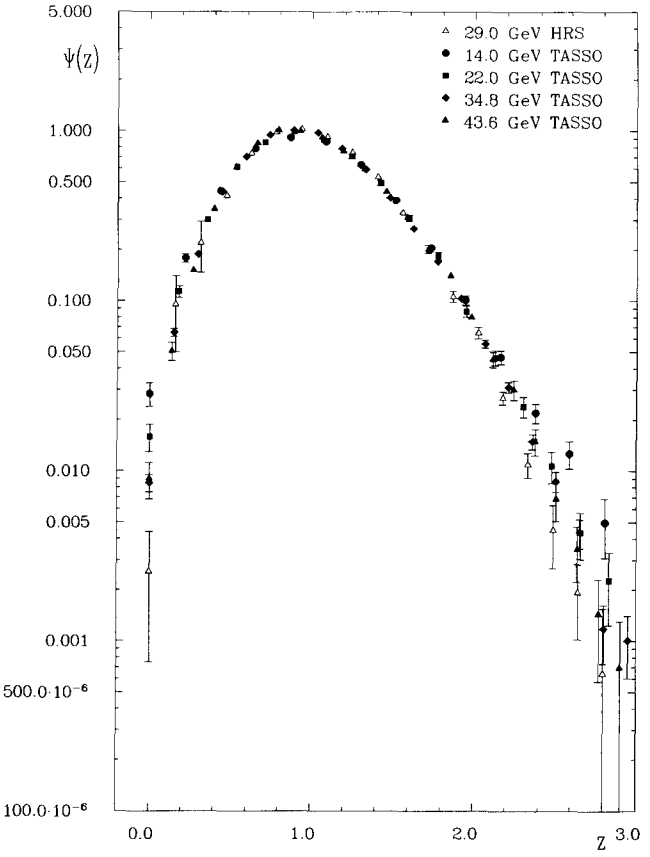

Fig. 9. Single hemisphere charged multiplicity distributions in KNO form

The approximate KNO-scaling is rather a surprising feature of the data since Feynman scaling was shown to be broken [1, 42] at the energies considered, invalidating the original basic assumption of [35]. In an attempt to solve this puzzle Bowler and Burrows studied [43] the multiplicity distributions generated by the Lund MC [44]. They showed that at low energies four-momentum conservation leads to narrowing of the multiplicity distributions. On the other hand, they observed that at higher energies production of b quarks and hard gluon emission increase the dispersion of the multiplicity distribution. These two effects, combined together, lead to proportionality between the mean value and the dispersion of the distributions and hence, to approximate KNO-scaling. They concluded that the apparent KNO-scaling observed in the data seems to be accidental rather than related to the fundamental dynamics.

8 Forward-backward multiplicity correlations

By forward-backward multiplicity correlations one means the correlations between the number of particles produced in the forward and in the backward hemisphere of an event. In hadronic data [45, 46] the average number of "forward" particles ($\langle n_F \rangle$) can be related to the number of "backward" particles (n_B) in the following way:

$$\langle n_F(n_B) \rangle = a + b \cdot n_B \tag{3}$$

where b measures the correlation strength and is positive for $\sqrt{s} > 10$ GeV and increases logarithmically with c.m.s. energy. It was also found that the correlations are stronger for particles with small rapidities ($|y| \leq 1$-"central" region) than for particles with large rapidities ($|y| > 1$). These experimental observations were qualitatively explained [47] within the framework of the multichain dual parton [48] and geometrical [49] models. Both these models predict values of b close to zero for lepton induced reactions. Indeed, in lepton-nucleon interactions no substantial forward-backward correlations were found [50]. Earlier, an analysis of these correlations was performed for e^+e^- annihilation data in our previous paper [2] at $\sqrt{s} = 34$ GeV and by the HRS Collaboration [19] at

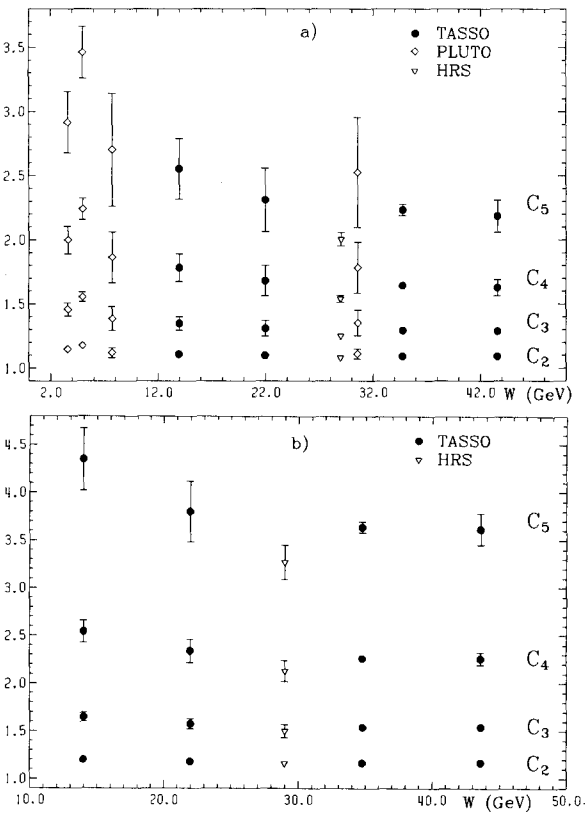

Fig.10. Energy dependence of C_l moments of: **a** whole event, **b** single hemisphere distributions

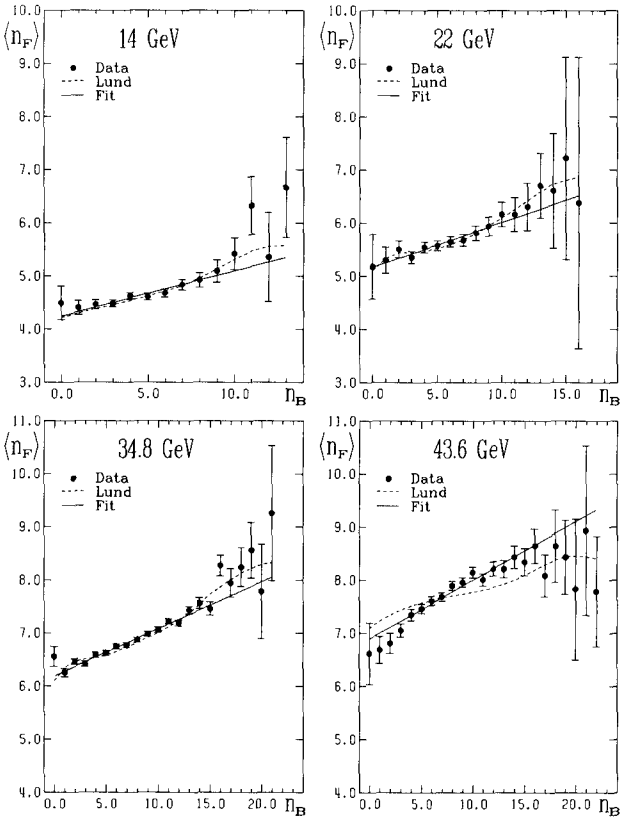

Fig. 11. The dependence of $\langle n_F \rangle$ on n_B for the full phase space data

$\sqrt{s}=29$ GeV. We found weak positive correlations in the full phase space and a slow rise of $\langle n_F \rangle$ with increasing n_B for the two rapidity intervals mentioned above with b larger in the central than in the outer region. HRS reported values of b consistent with zero for all regions. It should be pointed out that these correlations are very sensitive to the track and event selection criteria applied [2, 19].

The analysis of the forward-backward correlations was repeated, within the present study, using much larger statistics and the corrected multiplicity distributions. For the definition of the forward and backward hemisphere see Sect. 3. We defined the central (outer) region as: $|x_F| \equiv \left|\frac{2 \cdot p_l}{\sqrt{s}}\right| \leqq 0.15 \quad (|x_F| > 0.15)$, where p_l is the longitudinal component of the particle momentum w.r.t. the sphericity axis. The dependence of $\langle n_F \rangle$ on n_B at four energies together with predictions of the Lund model and the best fits of (3) is shown in Figs. 11 and 12. Values of the fitted slopes are listed in Table 7.

In all regions we observe weak, positive and approximately energy independent correlations, which are fairly well described by the linear relation (3). The correlations are the strongest in the central region. Values of the correlation strength b are smaller than those measured in hadron-hadron collisions at comparable energies. The Lund model [8] provides a good description of the observed dependences.

It was shown [2, 51] that the observed positive correlations may be at least partially explained by the interplay of the following: production of different quark flavours, their different fragmentation properties and by the production and decay of resonances. Since the agreement between the data and the Lund model is good, the influence of resonances and of heavier quarks can be studied using MC simulations. Results of these studies are presented in Fig. 13. The solid curve represents predictions of the Lund model for the final state particles. The dotted curve represents predictions for the final state particles in events initiated by u and d quarks. The removal of s, c and b quark events leads to a substantial decrease of the slope b. This shows that a large part of the observed correlations is due to the production of heavier quarks. It should be noted that the influence of these decreases with increasing $\sqrt{s}$. The dash-dotted curve represents predictions for the particles produced directly by the string fragmentation (primaries), i.e. before the resonances decayed, in events initiated by

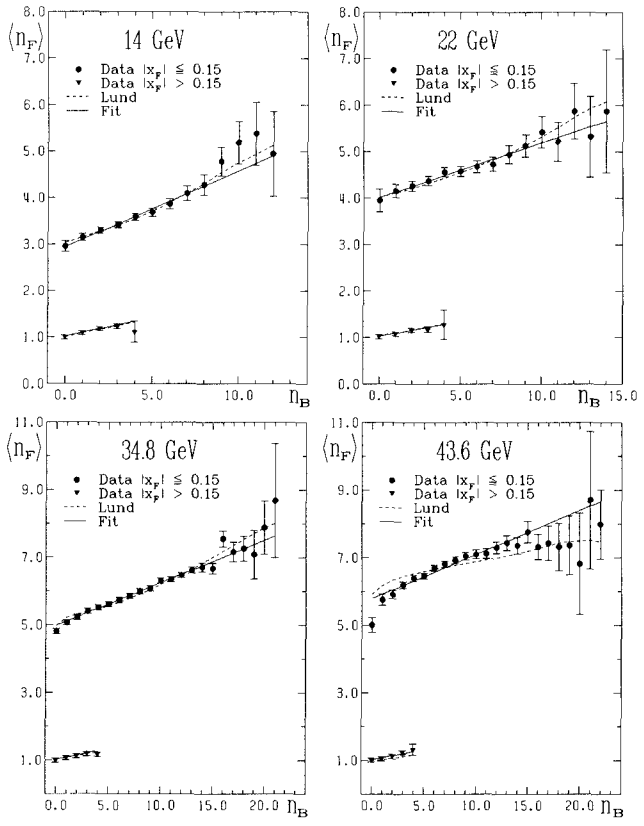

Fig. 12. The dependence of $\langle n_F \rangle$ on n_B for the central and outer region data

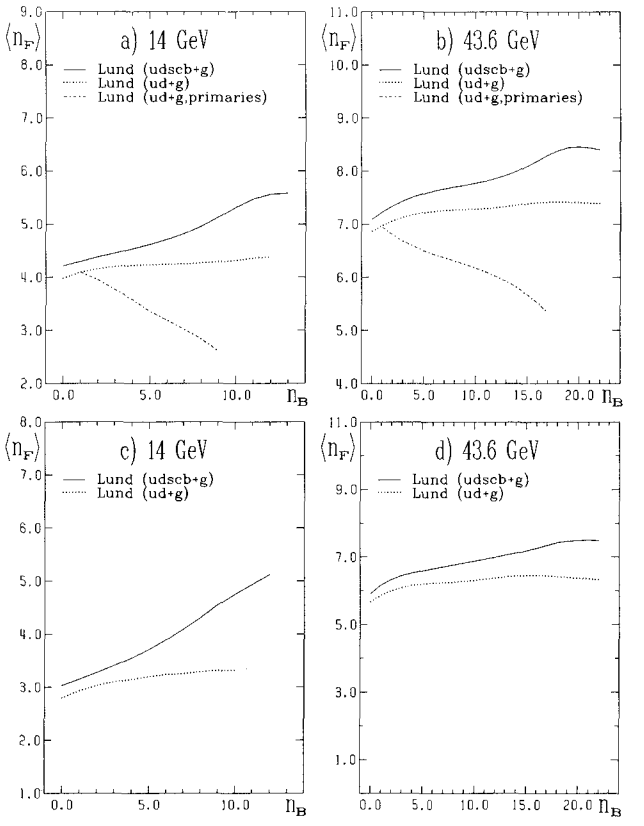

Fig. 13. The dependence of $\langle n_F \rangle$ on n_B. Monte Carlo studies. **a**, **b** – full phase space. **c**, **d** – central region

u and d quarks (Fig. 13a and b). As can be seen from these figures the primaries are anti-correlated. This anti-correlation is most probably due to the limited energy available. In the central region (Fig. 13c and d) the removal of s, c and b events leads to a substantial flattening of the distributions and has a similar energy dependence as was seen in the full phase space. We checked that in the outer kinematical region the effect of production of heavier quarks is negligible.

Recently, the NA22 Collaboration has published [46] results of the analysis of the forward-backward multiplicity correlations performed also for different particle charge selections i.e. between multiplicities of like and unlike charged particles. They found almost no correlations for the like charged particles $(+\,+, -\,-)$ and positive correlations for particles of opposite charges $(+\,-)$. It was argued [52] that e^+e^- annihilation data should show strong negative correlations for like sign particles and positive correlations of about the same strength for unlike sign particles.

An analysis of this type was repeated in the present study and its results are presented in Figs. 14 and 15 for the unlike and like sign particles, respectively. Values of the fitted slopes are listed in Table 8.

Indeed, the data for the unlike sign particles show positive correlations. They are strong and decreasing with c.m.s. energy. A different dependence of $\langle n_F \rangle$ on n_B is observed if the particles are of the same charges. The data (Fig. 15) show non-linear behaviour: a fast decrease of $\langle n_F \rangle$ for low values of n_B ($n_B \leqq 4$) and almost a constant value for $n_B > 4$. In the outer regions (not shown) the data exhibit very weak and approximately energy independent positive (negative) correlations if the considered particles are of different (same) charge. This suggests that the fastest particles in opposite hemispheres are more likely to be of opposite charge.

One should note that in both cases i.e. for unlike and like charged particles the Lund model provides a good description of the data.

Since this analysis deals with the charges of particles it is natural to ask what is the influence of overall charge conservation on the measured correlations. In order to estimate this effect a so called random charge model (RCM) was devised. In each generated event the charges of final state hadrons were randomised in such a way that the total charge was unchanged. The multiplicity of the event and the momenta of the particles were also unchanged. In this way the dynamical dependence on the particle charges except

Table 7. Fitted values of the correlation strength b

$\langle W \rangle$ (GeV)	Region					
	full		$\lvert x_F \rvert \leqq 0.15$		$\lvert x_F \rvert > 0.15$	
	b	$\frac{\chi^2}{N_{df}}$	b	$\frac{\chi^2}{N_{df}}$	b	$\frac{\chi^2}{N_{df}}$
14.0	0.085 ± 0.014	12/12	0.163 ± 0.014	6/11	0.081 ± 0.013	2/3
22.0	0.084 ± 0.016	4/15	0.117 ± 0.017	3/14	0.063 ± 0.016	1/3
34.8	0.089 ± 0.003	40/20	0.126 ± 0.003	23/20	0.064 ± 0.003	4/3
43.6	0.111 ± 0.009	20/21	0.131 ± 0.009	29/21	0.062 ± 0.009	5/3

Table 8. Fitted values of the correlation strength b for the unlike and like sign particles

$\langle W \rangle$ (GeV)	Region					
	full – unlike signs		$\lvert x_F \rvert > 0.15$ – unlike signs		$\lvert x_F \rvert > 0.15$ – like signs	
	b	$\frac{\chi^2}{N_{df}}$	b	$\frac{\chi^2}{N_{df}}$	b	$\frac{\chi^2}{N_{df}}$
14.0	0.306 ± 0.010	6.2/ 7	0.092 ± 0.013	0.4/2	-0.018 ± 0.013	0.1/2
22.0	0.251 ± 0.013	1.6/ 8	0.067 ± 0.017	0.2/2	-0.012 ± 0.016	0.1/2
34.8	0.226 ± 0.003	20.6/10	0.068 ± 0.003	1.8/2	-0.010 ± 0.003	0.1/2
43.6	0.200 ± 0.009	3.1/10	0.070 ± 0.009	0.8/2	-0.012 ± 0.009	0.1/2

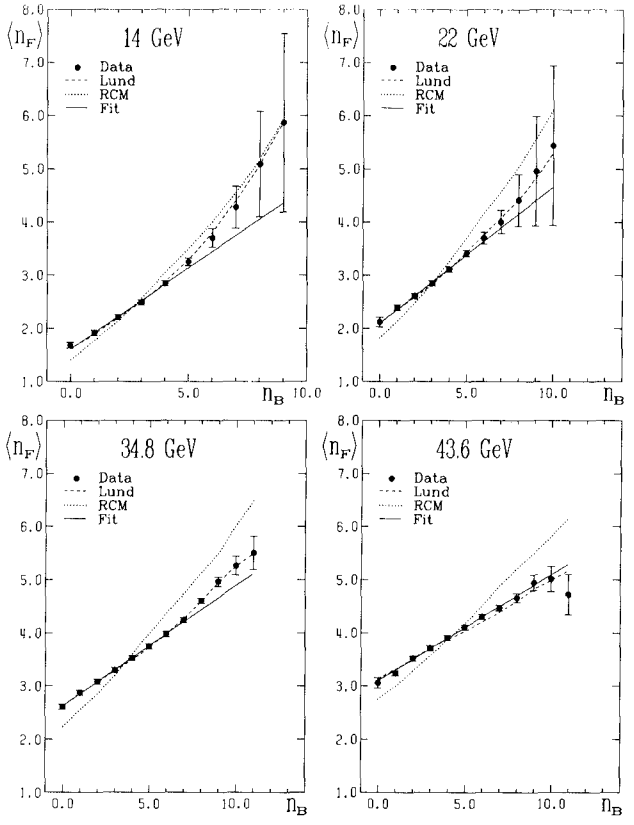

Fig. 14. The dependence of $\langle n_F \rangle$ on n_B for unlike sign particles in the full phase space

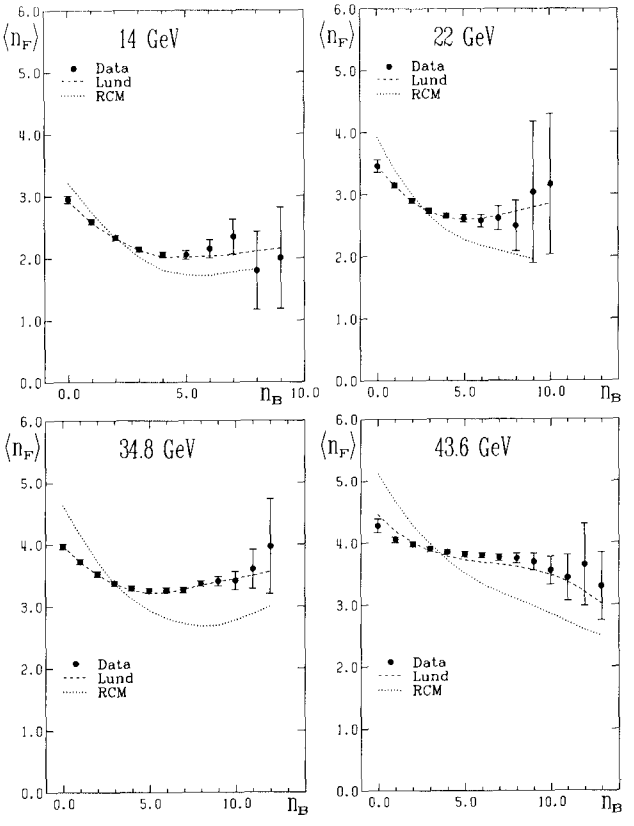

Fig. 15. The dependence of $\langle n_F \rangle$ on n_B for like sign particles in the full phase space

that from global charge conservation should get removed.

The comparison of the forward-backward correlations observed in the data, the Lund model and the RCM is shown in Figs. 14 and 15 for the full phase space. The RCM reproduces the trends observed in the data, but it predicts stronger correlations than measured. Differences between the data and RCM points become more pronounced with increasing $\sqrt{s}$. It seems that these differences can be qualitatively understood assuming the existence of a mechanism which minimizes the absolute value of the net charge ($Q_{B(F)}=n^{+}_{B(F)}-n^{-}_{B(F)}$) in a hemisphere. A good candidate for such a mechanism is local charge compensation which was found [2, 53, 54] to be responsible for strong short-range charge correlations.

It was checked with Monte Carlo simulation that the removal of events initiated by s, c and b quarks leads to stronger anti-correlations in the case of like charged particles, while in the case of unlike sign particles this removal results in a small flattening of the distributions.

9 Summary and conclusions

In the present paper the multiplicity distributions and correlations of charged particles produced in e^+e^- annihilation at centre of mass energies ranging from 14 to 46.8 GeV have been analysed.

The charged multiplicity distributions of whole events and of single hemispheres cannot be satisfactorily described by the Poisson distribution.

The negative binomial distribution can provide an acceptable description of the multiplicity distributions of whole event in limited central regions of the phase space, but it fails to describe either the multiplicity distributions of negatively charged particles or the one hemisphere multiplicity distributions. The energy and rapidity dependence of the shape parameter k of the negative binomial distribution follows the pattern observed in hadron-hadron and lepton-nucleon interactions.

Our multiplicity distributions show approximate KNO-scaling. However, the KNO scaled whole event charged multiplicity distributions cannot be described by the function proposed by Barshay and Yamaguchi.

The observed forward-backward multiplicity correlations are weak, positive and approximately energy independent. They are strongest in the central region. The correlations observed in e^+e^- annihilation are weaker than those measured in hadron-hadron collisions. As has been demonstrated in Monte Carlo studies, a substantial part of the correlations is due to production of heavier quarks. Also the production and decay of resonances have a strong influence. Effects of the quarks and resonances become less important with increasing energy. Forward-backward multiplicity correlations are charge dependent. They are strong and get weaker with energy and are positive (negative) if the considered particles are of different (same) charges. The charge dependence of forward-backward multiplicity correlations is to a large extent induced by the global charge conservation. The fact that they are weaker than those predicted by a model with randomized charges (satisfying global charge conservation) indicates that the charges of particles produced in the same hemisphere are likely to compensate. Anti-correlation for like sign particles is most probably due to limited energy available and hence, limited multiplicity. The observation of positive correlations for unlike charged particles, and negative correlations for like charged particles produced in outer regions supports a picture in which the fastest particles in different hemispheres carry opposite charges.

It should be stressed that forward-backward multiplicity correlations and their charge dependence are well reproduced by the Lund model. This shows that the qualitative features of the data can be understood in terms of this model, in particular resonance and heavy quark production and approximate local charge compensation as a consequence of the parton production and fragmentation processes.

Acknowledgements. We gratefully acknowledge the support of the DESY directorate, the PETRA machine group and the DESY computer centre. Those of us from outside DESY wish to thank the DESY directorate for the hospitality extended to us while working at DESY.

References

1. TASSO Coll., M. Althoff et al.: Z. Phys. C – Particles and Fields 22 (1984) 307
2. TASSO Coll., M. Althoff et al.: Z. Phys. C – Particles and Fields 39 (1985) 347
3. W. Kittel: Review Talk at the XVIII International Symposium on Multiparticle Dynamics, Tashkent, 1987
4. TASSO Coll., R. Brandelik et al.: Phys. Lett. 89B (1980) 418
5. TASSO Coll., R. Brandelik et al.: Phys. Lett. 83B (1979) 261; Z. Phys. C – Particles and Fields 4 (1980) 87
6. C. Youngman: Ph.D thesis, Imperial College, London, RL-HEP/T/82; H. Boerner et al.: Nucl. Instrum. Methods 176 (1980) 151; TASSO Coll., R. Brandelik et al.: Phys. Lett. 113B (1982) 499
7. P.D. Dauncey: Oxford D. Phil. thesis, RAL T 034 (1986); P.N. Burrows: Oxford D. Phil. thesis, RAL T 071 (1988)
8. B. Anderson, G. Gustafson, T. Sjöstrand: Phys. Lett. 94B (1980) 211; Z. Phys. C – Particles and Fields 6 (1980) 235; Nucl. Phys. B197 (1982) 45; T. Sjöstrand: Comp. Phys. Commun. 39 (1986) 347; Comp. Phys. Commun. 28 (1983) 229; Comp. Phys. Commun. 27 (1982) 243
9. G. Marchesini, B.R. Webber: Nucl. Phys. B238 (1984) 1; B.R. Webber: Nucl. Phys. B238 (1984) 492
10. S.L. Lloyd, B. Foster: SIMPLE writeup, unpublished
11. D.G. Cassel, H. Kowalski: Nucl. Instrum. Methods 185 (1981) 235

12. TASSO Coll., W. Braunschweig et al.: Z. Phys. C – Particles and Fields 41 (1988) 353
13. TASSO Coll., W. Braunschweig et al.: DESY 88–173 (1988); TASSO Coll., M. Althoff et al.: Z. Phys. C – Particles and Fields 27 (1985) 27; I.R. Tomalin: Oxford D. Phil. thesis, RAL T 069 (1988); TASSO Coll., W. Braunschweig et al. Z. Phys. C – Particles and Fields 42 (1989) 189; TASSO Coll., M. Althoff et al.: Z. Phys. C – Particles and Fields 17 (1983) 5; H.L. Krasemann: Ph. D thesis, DESY Internal Report F35-85-02 (1985)
14. C. Bacci et al.: Phys. Lett. 86B (1979) 234
15. LENA Coll., B. Niczyporuk et al.: Z. Phys. C – Particles and Fields 9 (1981) 1
16. MARK I Coll., J.L. Siegrist et al.: Phys. Rev. D26 (1982) 969
17. PLUTO Coll., Ch. Gerke: Private Communication. Data collected at $\sqrt{s}$=3.61, 5.0, 7.73, 9.39, 12.0, 13.0, 16.98. 22.02, 27.53 and 30.58 GeV
18. JADE Coll., W. Bartel et al.: Z. Phys. C – Particles and Fields 20 (1983) 187
19. HRS Coll., M. Derrick et al.: Phys. Lett. 168 B (1986) 299; Phys. Rev. D 34 (1986) 3304
20. W. Thome et al.: Nucl. Phys. B129 (1977) 365
21. H. Satz: Lecture Notes in Physics, p. 49, Berlin, Heidelberg, New York: Springer 1976
22. W. Furmański, R. Petronzio, S. Pokorski: Nucl. Phys. B155 (1979) 253
23. A. Bassetto, M. Ciafaloni, G. Marchesini: Phys. Lett. 83 B (1979) 207; K. Konishi: Rutherford Report RL 79-035 (1979); A.H. Mueller: Phys. Lett. 104 B (1981) 161; Nucl. Phys. B213 (1983) 85
24. P. Carruthers, C.C. Shih: Int. J. Mod. Phys. A 2 (1987) 1447
25. M.L. Perl: High energy hadron physics. New York: Wiley 1974
26. M. Bengtsson, T. Sjöstrand: Phys. Lett. 185 B (1987) 435; T, Sjöstrand, M. Bengtsson: Comp. Phys. Commun. 27 (1982) 243
27. M. Garetto, A. Giovannini: Lett. Nuovo Cimento 7 (1973) 35; A. Giovannini et al.: Nuovo Cimento 24A (1974) 421; N. Suzuki: Prog. Theor. Phys. 51 (1974) 1629
28. W.J. Knox: Phys. Rev. D10 (1974) 65
29. B. Åsman: Ph. D. thesis, University of Stockholm, Stockholm 1985
30. UA5 Coll., G.J. Alner et al.: Phys. Lett. 160 B (1985) 193; Phys. Lett. 160 B (1985) 199; Phys. Lett. 167 B (1986) 476
31. NA 22 Coll., M. Adamus et al.: Z. Phys. C – Particles and Fields 32 (1986) 475; Phys. Lett. B 177 (1986) 239; Z. Phys. C – Particles and Fields 37 (1988) 215; F. Meijers: Ph. D. thesis, University of Nijmegen, ISBN 90-90001615-5, 1987
32. EMC Coll., M. Arneodo et al.: Z. Phys. C – Particles and Fields 35 (1987) 335
33. NA5 Coll., F. Dengler et al.: Z. Phys. C – Particles and Fields 33 (1986) 187; EHS-RCBC Coll., J.L. Bailly et al.: Z. Phys. C – Particles and Fields 40 (1988) 215
34. R. Szwed, G. Wrochna, A.K. Wróblewski: Acta Phys. Pol. B19 (1988) 763
35. Z. Koba, H.B. Nielsen, P. Olesen: Nucl. Phys. B40 (1972) 317
36. A. Białas, F. Hayot: Phys. Rev. D33 (1986) 39
37. Chao Wei-qin, Meng Ta-chung, Pan Ji-cai: Phys. Rev. D35 (1987) 152; Phys. Lett. B176 (1986) 211
38. K. Fiałkowski: Phys. Lett. B169 (1986) 436; Phys. Lett. B173 (1986) 197
39. R.P. Feynman: Phys. Rev. Lett. 23 (1969) 1415
40. UA5 Coll., G.J. Alner et al.: Phys. Lett. 138 B (1984) 304
41. S. Barshay, Y. Yamaguchi: Phys. Lett. B51 (1974) 376
42. MARK II Coll., J.F. Patrick et al.: Phys. Rev. Lett. 49 (1982) 1232
43. M.G. Bowler, P.N. Burrows: Z. Phys. C – Particles and Fields 31 (1986) 327
44. T. Sjöstrand: Comp. Phys. Commun. 28 (1983) 229
45. C. Bromberg et al.: Phys. Rev. D9 (1974) 1864; T. Kafka et al.: Phys. Rev. Lett. 34 (1975) 687; H. Gräsler et al.: Nucl. Phys. B90 (1975) 401; S. Uhlig et al.: Nucl. Phys. B132 (1978) 15; J.W. Lämsä et al.: Phys. Rev. D18 (1978) 3933; R. Göttgens et al.: Z. Phys. C – Particles and Fields 11 (1981) 189; V. Grishin et al.: Yad. Fiz. 43 (1986) 609; V.M. Kubik et al.: Yad. Fiz. 43 (1986) 89; UA5 Coll., K. Alpgard et al.: Phys. Lett. 123 B (1983) 361; UA5 Coll.: Charged particle correlations in $p\bar{p}$ collisions at c.m. energies of 200, 546 and 900 GeV, submitted to Z. Phys. C – Particles and Fields
46. P. Van Hal: Ph. D. thesis, University of Nijmegen, ISBN 90-90001537, 1987; NA22 Coll.: Forward-backward multiplicity correlations in $\pi^+ p$, $K^+ p$ and pp collisions at 250 GeV/c. To be published
47. K. Fiałkowski, A. Kotański: Phys. Lett. 115 B (1982) 425; A. Capella, J. Tran Thanh Van: Z. Phys. C – Particles and Fields 18 (1983) 85; A. Capella, A. Krzywicki: Phys. Rev. D18 (1978) 4120
48. G. Veneziano: Nucl. Phys. B117 (1976) 519; A. Capella et al.: Z. Phys. C – Particles and Fields 3 (1980) 329
49. S. Barshay: Z. Phys. C – Particles and Fields 32 (1986) 513; S.Barshay, E. Eich: Phys. Lett. B178 (1986) 431; S. Barshay: Phys. Lett. B42 (1972) 457
50. H. Gräsler et al.: Nucl. Phys. B223 (1983) 269; EMC Coll., M. Arneodo et al.: Nucl. Phys. B258 (1985) 249
51. W. Koch: Proceedings of the XIII International Symposium on Multiparticle Dynamics, Volendam 1982, p. 534
52. S. Barshay: Phys. Lett. 199 B (1987) 121
53. TASSO Coll., R. Brandelik et al.: Phys. Lett. 100 B (1981) 357
54. CLEO Coll., S. Berends et al.: Phys. Rev. D31 (1985) 2161